Hindawi

Research Article

Analysis of the Mineral Compositions of Lateritic Clay in Guangxi and their Influence

Er-jing Yang [1,2,3] **Sha-sha Zeng** [2] **Hong-yan Mo** [2] **Cheng-lin Yang** [2]
Cheng Chen [1,3] **and Yan-fu Wang** [4]

[1]*Yellow River Conservancy Technical Institute, Kaifeng 475004, China*
[2]*School of Civil Engineering and Architecture, Guilin University of Technology, Guilin 541004, China*
[3]*Henan Engineering Research Center of Eco-hydraulic for Small Watershed, Kaifeng 475004, China*
[4]*School of Civil Engineering and Architecture, Guangxi University, Nanning 530004, China*

Correspondence should be addressed to Sha-sha Zeng; zengshasha2016@163.com and Hong-yan Mo; mohongyan@glut.edu.cn

In order to study the effect of mineral composition on the physical properties of lateritic clays, the mineral compositions of four kinds of lateritic clay from Guangxi province in China were quantitatively analyzed by means of DTA, XRD, SEM, XRF and total chemical element analysis. On this basis, the variation law of macroscopic physical properties of lateritic clay was analyzed from the perspective of mineralogy. The results show that kaolinite and goethite are the main minerals of lateritic clays from Guangxi in China. The mineral compositions of these four samples are quantitatively and accurately analyzed by Bogue's method. According to the study on mineral compositions of soil samples, the physical properties of lateritic clay are related to its clay minerals and cemented substances. The liquid limit (LL) or plastic limit (PL) increases with the increase of the ability and content of clay minerals to adsorb water. The lateritic clay is dominated by kaolinite minerals with low adsorption capacity, so the observed boundary water content (LL and PL) of high value of lateritic clays can be explained by the contribution of "inert water" in soil pores. The iron-bonded cement minerals (the form of existence is goethite) in lateritic clay have great influence on the liquid and plastic limits, which decrease linearly with the increase of goethite, whereas the goethite has relatively smaller effect on shrinkage characteristics. It is believed that the shrinkage characteristics of lateritic clay may also be affected by other factors.

1. Introduction

Undisturbed lateritic clay has good mechanical properties but poor physical properties. It is widely distributed in Guangxi province of China [1–5], especially in Guilin, Liuzhou, Laibin and Wuming. In recent years, due to the extreme climate in China, engineering diseases such as slope instability, uneven settlement of foundations and cracking of embankments [6, 7] have occurred frequently in lateritic clays. Due to the strong hydrophilic nature of lateritic clay, the physical-mechanical property changes caused by soil-water action are very complex, and the mineral composition as the main carrier is the material basis to explain the changes in its relevant physical-mechanical properties. In the 1950s, Norrish [8] studied the expansibility of montmorillonite

crystals. Tan [9] studied the expansion and contraction mechanism of montmorillonite crystal, and discussed the relationship between the crystal plane spacing of montmorillonite and the type and concentration of electrolyte solution. Tan and Kong [10] studied the expansion and contraction laws of montmorillonite crystals, and analyzed the reasons for the different expansion and contraction characteristics of unsaturated montmorillonite crystals. Wang [11] first studied the cementation of lateritic clay and discussed the influence of free iron oxide on the engineering properties of lateritic clay. The results show that the engineering mechanical properties of lateritic clay are close to ordinary clay after removing free iron oxide. Kong et al. [12] further studied the cementation characteristics of lateritic clay, and the results show that only a part of free iron oxide

really plays the role of cementation. The above research shows that the mineral composition has a significant impact on the physical and mechanical properties of soil.

For a long time, scholars at home and abroad have done a lot of research on the composition and microstructure of clay minerals and cementitious substances in soils [13–17]. In terms of quantitative analysis of mineral composition, Tan [18] used a simplified algorithm for quantitative analysis of clay minerals. Zhang and Fan [19] quantitatively analyzed clay minerals by X-ray diffraction phase quantitative method. Dai et al. [20] first qualitatively identified the mineral composition by X-ray diffraction, and then quantitatively analyzed the content of mineral composition according to the intensity and half height width of diffraction peak. However, the above quantitative analysis methods have their own limitations.

In this paper, the mineral composition of four kinds of lateritic clay in Guangxi province of China is qualitatively identified and quantitatively analyzed by means of differential thermal analysis(DTA), X-ray diffraction(XRD), scanning electron microscope(SEM), X-ray fluorescence analysis(XRF) and full chemical element analysis. On this basis, the influence law of mineral compositions on the physical properties of lateritic clay is revealed. This research provides a new way to further study the engineering characteristics and genesis of lateritic clay in this area.

2. Soil Samples

The test soil samples were taken from four typical distribution areas of lateritic clay in Guangxi province of China as follows: Guilin, Liuzhou, Laibin and Wuming, numbered as S-1, S-2, S-3, and S-4, respectively. After indoor geotechnical tests, the basic physical property indexes of the four lateritic clay specimens are shown in Table 1 [21].

3. Testing Methods

3.1. Qualitative Analysis of Mineral Composition. Clay minerals in clayey soils are mainly present in the colloidal (less than 2 μm) group, therefore, the separation/preparation of colloidal particles in soil samples needs to be carried out in advance by physicochemical methods before the experiments [22, 23], and the specific experimental steps are as follows.

(i) According to the required amount of sample, weigh the air-dried sample with particle size less than 0.075 mm and place it in a small beaker for wetting and standby.

(ii) Add hydrochloric acid solution with the concentration of 0.1 mol/L, fully stir to completely decompose carbonate or other soluble salts in the soil sample, and discard the upper part by decantation method after static clarification.

(iii) Continue to treat the sample with dilute hydrochloric acid with $pH = 4$ to remove calcium and magnesium ions from the filtrate.

(iv) Place the treated sample in a constant temperature water bath at 40°C, add 30% H_2O_2 and stir continuously to remove the organic matter in the soil sample.

(v) Add sodium citrate buffer, heat it to 80°C in a constant temperature water bath, add sodium bisulfite in several times and stir fully to remove the iron cement in the sample.

(vi) After adding 2% sodium carbonate solution for dispersion treatment, separate the colloidal particles of the treated sample by densitometer method, and finally dry the separated sample for standby.

3.1.1. Differential Thermal Analysis (DTA) Test. Extract samples from Wuming (less than 2 μm particle size) for DTA test. Labsys synchronous thermal analyzer produced by Setaram Company of France is used for the test. The test conditions are as follows: the temperature rises from room temperature to 1000°C, the heating rate is 10°C/min, the cooling rate is 50°C/min, and the test reference sample is pure Al_2O_3.

3.1.2. X-ray Diffraction (XRD) Analysis Test. X-ray diffraction analysis (XRD) is widely used for the identification of clay minerals and the study of their crystal structure. The principle is based on the fact that different minerals have different crystalctures; the powder crystal method was used for the qualitative analysis of the four soil samples mentioned above. The following conditions were used: tube voltage 40 kV, tube current 40 mA, initial angle 4°, termination angle 32°, scanning rate 6°/min, angle 0.0170°(2θ) per step and test temperature 25°C. The test was carried out using an X-Pert PRO X-ray diffractometer from PANalytical B. V.

3.1.3. Scanning Electron Microscope (SEM) Test. Microstructural observations were carried out on the raw and extracted samples (colloidal particles smaller than 2 μm) of the four lateritic clays mentioned above with the aid of a scanning electron microscope to analyze the morphology of the mineral constituents and the way in which the particles lap each other. Quanta-200 scanning electron microscope was used in the test. The test conditions are as follows: the resolution of dry sample under high vacuum 30 kV environments is 3.5 nm, and that of water sample under low vacuum 3 kV is 15 nm.

3.2. Quantitative Analysis of Mineralogical Composition. In this paper, the Bogue method was used for the quantitative analysis of mineral compositions. A prerequisite for the successful application of this method is the accurate acquisition of chemical elemental results for the minerals. X-ray fluorescence analysis (XRF) and full chemical elemental analysis experiments were used to determine the elements contained in the four soil samples.

TABLE 1: Physical indices of soil samples [21].

Sample number	Depth/m	Water content/%	Density/ (g·cm^{-3})	Liquid limit/%	Plastic limit/%	Plastic index	Free swelling rate/%	Line shrinkage rate/%	Volume shrinkage rate/%	Shrinkage coefficient
S-1(Guilin)	2.0 ~ 4.0	34.9	1.85	70.3	39.8	30.5	35.0	3.52	9.65	0.35
S-2(Liuzhou)	0 ~ 3.0	42.4	1.78	72.6	45.9	26.7	19.0	4.51	12.54	0.37
S-3(Laibin)	2.0 ~ 3.0	41.0	1.64	82.0	46.2	35.8	21.5	3.63	17.98	0.34
S-4(Wuming)	0 ~ 3.0	34.3	1.70	83.0	54.1	28.9	39.0	0.38	3.68	0.21

X-ray fluorescence analysis (XRF) test: This is a method of qualitative and quantitative analysis of elements using X-ray excitation of the sample to produce characteristic fluorescence spectral lines with high accuracy for the analysis of elements. In this paper, an Axios X-ray fluorescence analyzer (PANalytical B. V.) was used. The test conditions were as follows: radiation source is Rh target; radiation tube is 2.4 kW; fused sheet method is for the sample; and atomic absorption spectrometry is for the determination of carbon.

Full chemical element analysis test: The test was completed in the material experiment center of Guilin University of technology. SiO_2, Al_2O_3, Fe_2O_3, Cao, MgO, K_2O, Na_2O, MnO and other elements were measured in the sample.

The Bogue method assumes that: ①Only the phases analyzed by the X-diffraction test are present in the soil sample and other trace minerals are ignored, i.e., the sum of mineral contents analyzed by X-ray diffraction test is 100%; ②If a mineral contains an element, but other minerals do not contain the element, the element can be used to determine the content of the mineral in the soil sample [17, 24]. Based on these two assumptions, using the molecular weight of the element, the theoretical molecular weight of the mineral and the measured elemental content, (1) can be formulated to find the content of each mineral in the soil sample.

$$\left.\begin{array}{l} a_1 x + b_1 y + c_1 z = A \\ a_2 x + b_2 y + c_2 z = B \\ a_3 x + b_3 y + c_3 z = C \end{array}\right\}, \quad (1)$$

Where, a, b, c are the equation coefficients, respectively, whose values are the ratio of the molecular weight of the element to the theoretical molecular weight of the mineral containing the element; x, y, z are the percentage content of the mineral sought, respectively; and A, B, C are the percentage content of the measured element, respectively.

4. Testing Results and Analysis

4.1. Qualitative Analysis Results

4.1.1. Differential Thermal Analysis Tests. The DTA curve of Wuming lateritic clay (S-4) is shown in Figure 1. It can be seen that Wuming sample has endothermic reaction at 250–300°C, with medium intensity endothermic peak, strong endothermic peak at 500–550°C and obvious exothermic peak at about 950°C. A check of the Handbook of Differential Thermal Analysis for Mineral Identification [25] revealed that the first heat-absorbing peak was characteristic for gibbsite. By analogy, kaolinite-like minerals are also
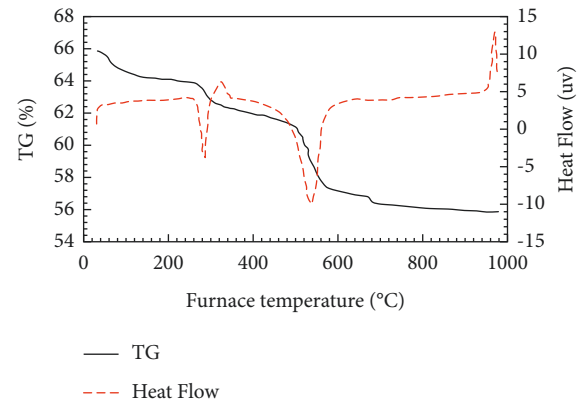

FIGURE 1: DTA curves of S-4 (Wuming).

present in the Wuming sample. The kaolinite-like minerals may be one or more of kaolinite/ellite/iron ellite, but ellite, iron ellite would have a clear valley of heat absorption reaction between 100 and 200°C, which is clearly inconsistent with the results in Figure 1, from which it can be inferred that the kaolinite-like minerals are kaolinite.

4.1.2. X-ray Diffraction Test. The X-ray diffraction curves of Wuming samples with different particle groups are shown in Figure 2. It can be seen from Figure 2 that there are three obvious peak lines in Wuming sample, d_0 are 7.15 Å, 3.58 Å and 4.8 Å, respectively. In fact, 7.15 Å and 3.58 Å are typical characteristic peaks of kaolinite [26], so it can be concluded that kaolinite exists in Wuming sample. While 4.8 Å is a characteristic peak of gibbsite, which leads to the preliminary conclusion that gibbsite is present in the Wuming sample. Comparison of Figures 2(a) and 2(b) shows that the diffraction curves of the original sample and the sample smaller than 75 μm are basically the same, indicating that the particles smaller than 75 μm are predominant in the Wuming sample. In addition, Figure 2(c) shows that the 4.17 Å peak line is missing from the curve of the less than 2 μm sample compared to the original sample and the less than 75 μm sample. In other words, the 4.17 Å peak line is also present in the Wuming sample, which is a characteristic peak for goethite. Goethite is usually red, but the sample less than 2 μm is white, i.e. no needle iron ore is present, indicating that goethite has been removed, whereas the original sample and the less than 0.075 mm soil sample are mainly red, indicating the presence of goethite in both. Comparison of the results of the differential thermal analysis of the Wuming sample shows that the results of the
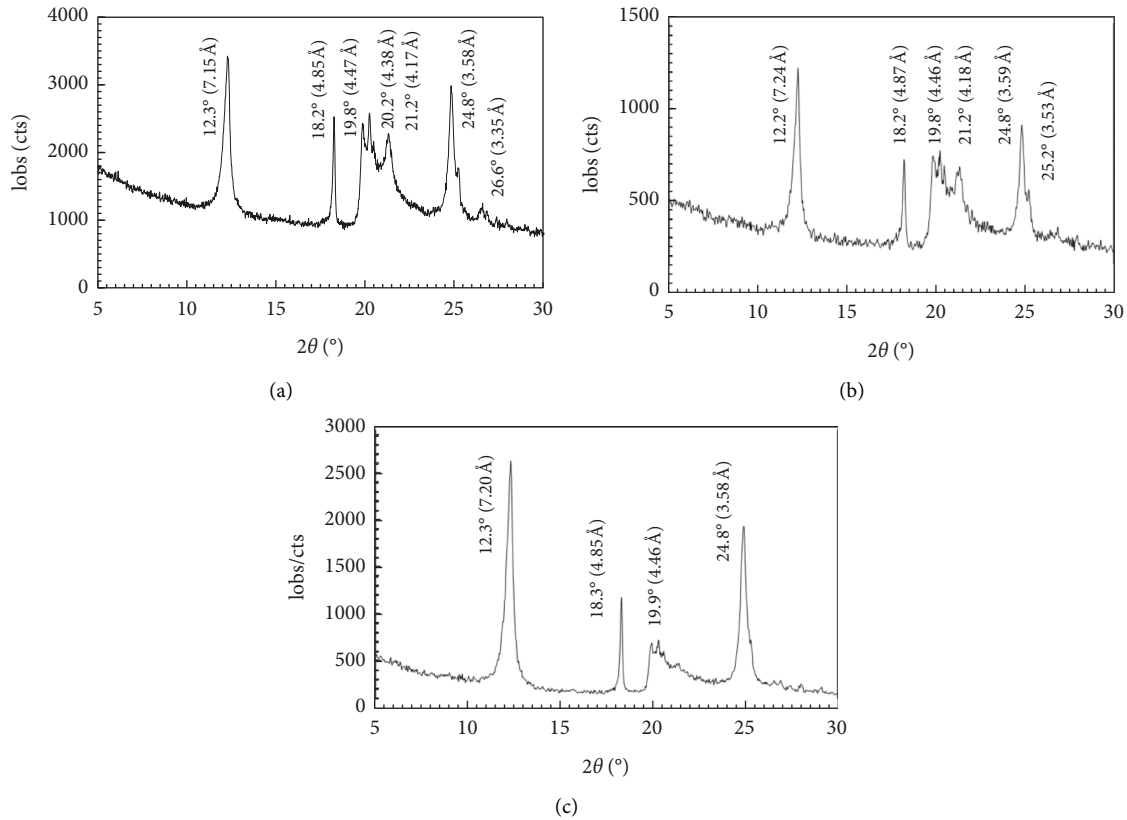
(a)

(b)

(c)

FIGURE 2: XRD curves of S-4 (Wuming). (a) Original sample. (b) Sample less than $75\,\mu$m. (c) Sample less than $2\,\mu$m.

differential thermal analysis are in general agreement with the results of the X-ray diffraction analysis.

Figure 3 shows the diffraction curves for S-1, S-2, and S-3. The analysis process was the same as for S-4, i.e. the identification of mineral species was completed by comparing the results of the differential thermal analysis tests with the measured X-ray diffraction curves. Overall, the differential thermal analysis (DTA) and X-ray diffraction (XRD) tests were able to determine the main mineral composition of the soil samples from each location, and the results are summarized in Table 2.

4.1.3. Scanning Electron Microscope Test.

The SEM image of Wuming sample is shown in Figure 4. It can be seen that the mineral crystals in the original Wuming sample are hairy spherical and cementitious structure. Because the Wuming sample is wrapped by free iron oxide, it is difficult to see the type and connection mode of internal micro units. The micro units in the extracted samples are irregular flakes, with different thickness and size, scattered accumulation and disorderly arrangement. The dissolved water sample expands due to water absorption, the flake particles increase, the micro unit is hexagonal, the contour is clear, the thickness is uniform, the edges are obvious, and the flake basic units are in face-to-face contact and superimposed together, which is a typical feature of kaolinite. In conclusion, the experimental results of DTA, XRD and SEM are consistent with each other.

4.2. Quantitative Analysis Results of the Bogue Method.

The results of the XRF analysis and the full chemical elemental analysis are shown in Tables 3 and 4, respectively, and the comparison shows that the results of the two chemical elemental analysis methods for the same elemental mass percentages are basically the same, indicating that the results of the chemical elemental analysis of the above four lateritic clays are reliable.

Due to space limitations, this paper only takes S-4 (Wuming lateritic clay) as an example to briefly introduce the process of quantitative analysis of mineral components in soil by Bouge method. It can be seen from Table 2 that the mineral components of Wuming lateritic clay are kaolinite, gibbsite and goethite. Table 5 shows the content and theoretical molecular weight of various elements in S-4 (The measured element content is taken from the XRF analysis test). According to formula (1) and Table 5, the mass percentages of kaolinite, gibbsite and goethite can be calculated, respectively, as follows.

Goethite:

$$8.53\% \times \frac{79 \times 2}{160} = 9.49\%. \tag{2}$$

Kaolinite:

$$36.48\% \times \frac{258}{60 \times 2} = 78.43\%. \tag{3}$$

Gibbsite:

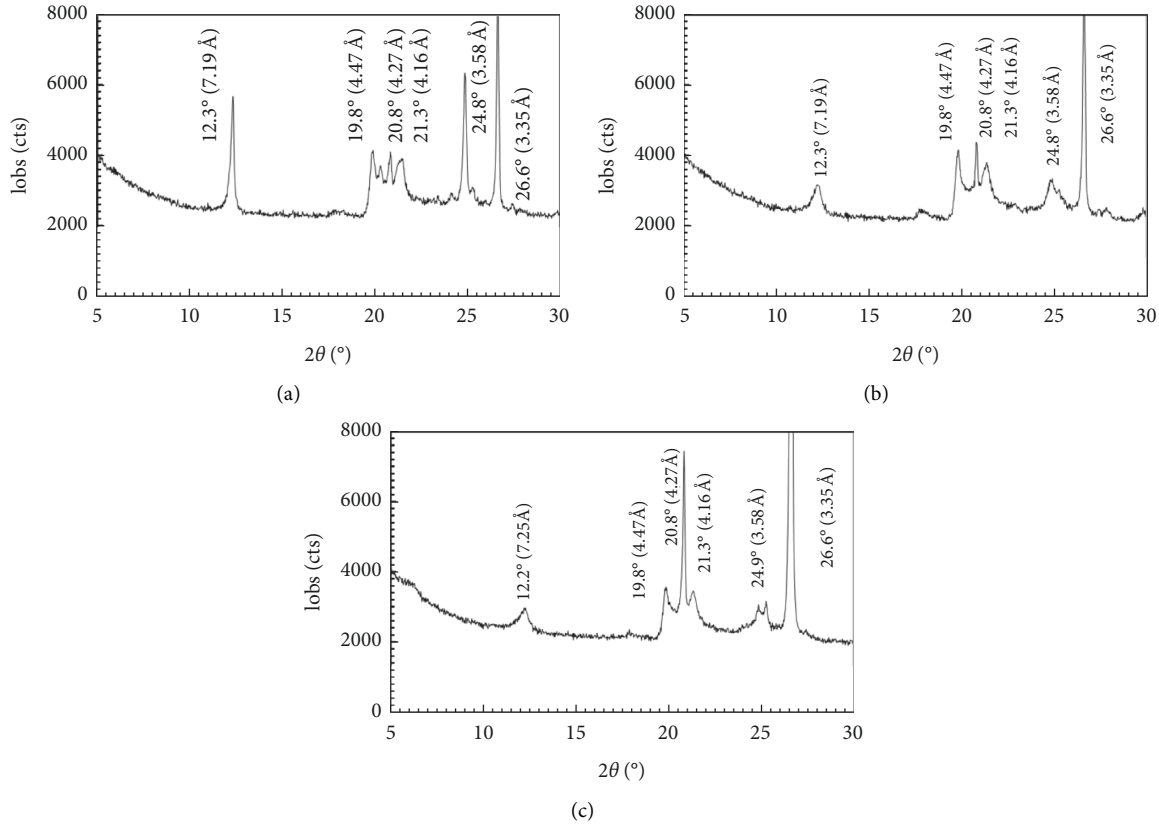$$1 - 78.43\% - 9.49\% = 12.08\%. \tag{4}$$

(a)

(b)

(c)

FIGURE 3: XRD curves of S-1 ∼ S-3. (a) Original sample of S-1(Guilin). (b) Original sample of S-2(Liuzhou). (c) Original sample of S-3(Laibin).

TABLE 2: Main mineral compositions of lateritic clay samples.

Sample number	Mineral compositions
S–1 (Guilin)	Quartz, kaolinite, goethite
S–2 (Liuzhou)	Quartz, kaolinite, goethite, calcite
S–3 (Laibin)	Quartz, kaolinite, goethite
S–4 (Wuming)	Kaolinite, goethite, gibbsite

Deviation of Al_2O_3:

$$37.32\% - \left(78.43\% \times \frac{102}{258} + 12.08\% \times \frac{102}{78 \times 2}\right) = -1.59\%. \tag{5}$$

By analogy, based on the data of the elemental content measured by full chemical elemental analysis and XRF, the mineral composition content in various samples can be calculated by the Bogue method respectively, and the calculation results and error analysis are summarized in Tables 6 and 7, respectively.

As can be seen from Table 7, for the Wuming lateritic clay (S-4), the error values for the percentage mineral content solved from the results of the full chemical elemental analysis method are relatively small, and the error in the results solved by the XRF method is also small. This is due to the relatively small number and single type of major mineral components in the Wuming lateritic clay, which results in an overall small error.

4.3. Influence of Mineral Composition on the Physical Properties of Lateritic Clay

4.3.1. Influence of Kaolinite on Atterberg's Limits. Figure 5 shows the relationship between kaolinite content (as listed in Table 6) and the Atterberg's limits (liquid limit LL and plastic limit PL, which as listed in Table 1) of the four lateritic clays mentioned above. It can be seen from Figure 5 that the correlation between kaolinite and the Atterberg's limits is very weak; However, the values of liquid limit (LL) and plastic limit (PL) are generally rather high. According to the electric double layer theory [27–32], strongly bound water is the adsorbed water layer under the action of particle surface adsorption energy, and weakly bound water is the permeable water layer between diffusion layer and free liquid under osmotic pressure [33–35]. The more the surface charges of clay minerals, the stronger the adsorption energy, the thicker the adsorbed water layer, and the more strongly and weakly bound water. The research shows that there is an obvious correlation between strongly bound water - plastic limit (PL) and weakly bound water - liquid limit (LL) [36–38]. Because the lateritic clays are dominated by kaolinite minerals with low adsorption capacity, this better explains the weak correlation between kaolinite and the Atterberg's limits (PL and LL). Xue and Bian [39] pointed out that the pores in lateritic clay are mainly closed or semi closed small pores, and the water in these small pores is often
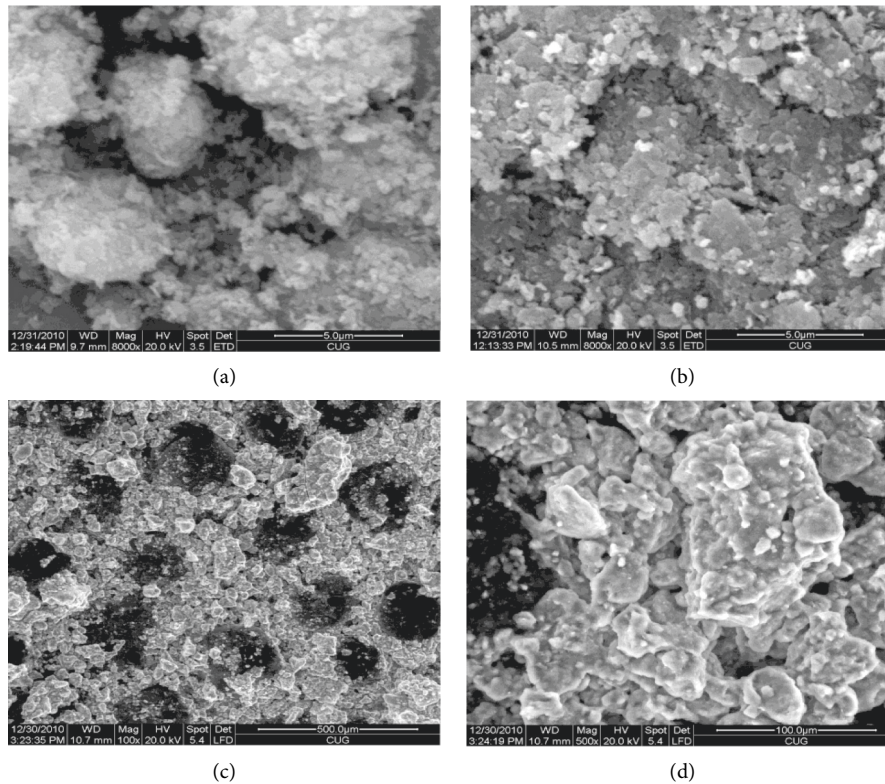
(a)

(b)

(c)

(d)

FIGURE 4: SEM photographs of samples in Wuming. (a) Original sample (×8000) (b) Extract sample (×8000). (c) Original sample dissolved water (×100) (d) Original sample dissolved water (×500).

TABLE 3: Analytical results by XRF tests.

Sample number	Mass percentage of chemical elements/%			
	SiO_2	Al_2O_3	Fe_2O_3	SiO_2/Al_2O_3
S–1 (Guilin)	41.96	28.12	14.85	1.492
S–2 (Liuzhou)	42.6	27.91	12.85	1.526
S–3 (Laibin)	58.61	18.50	10.64	3.168
S–4 (Wuming)	36.48	37.32	8.53	0.977

TABLE 4: Analytical results by chemistry element analysis tests.

Sample number	Mass percentage of chemical elements/%			
	SiO_2	Al_2O_3	Fe_2O_3	SiO_2/Al_2O_3
S–4 (Wuming)	36.27	37.71	8.66	0.962

TABLE 5: Content of element and molecular weight of S-4.

Mineral compositions	Kaolinite	Goethite	Gibbsite
Theoretical molecular weight	258	89	78
Measured element	SiO_2	Fe_2O_3	Al_2O_3
Theoretical molecular weight	60	102	160
Mass percentage of measured elements/%	36.48	37.32	8.53

called "inert water", whose character is similar to weakly bound water. Therefore, the authors believe that the relatively high liquid and plastic limits of lateritic clay are related to the existence of "inert water" in pores.

4.3.2. Influence of Kaolinite on the Expansibility. Figure 6 shows the relationship curve between kaolinite content (as listed in Table 6) and the free swelling rate (as listed in Table 1) of the four lateritic clays. As can be seen from Figure 6, the correlation between kaolinite content in lateritic clays and its free swelling rate is rather weak. From the results of the qualitative and quantitative analysis of the mineral composition, it can be seen that the kaolinite content of the lateritic clay specimens is basically above 70%, but the kaolinite is not entirely present in a loose state of clay particles, and some of the kaolinite is wrapped by ferric substances, forming larger agglomerates of agglomerates. Scanning electron microscope (SEM) analysis shows that the encapsulated kaolinite tends not to swell or swells very weakly (see Figure 4). In addition, due to the weaker lattice substitution ability of kaolinite, the particles have relatively little surface charge and are less able to adsorb water molecules. This could better explain the relatively low free swelling of lateritic clay and the weak correlation with kaolinite content.

4.3.3. Influence of Goethite on Physical Properties of Lateritic Clay. Figure 7 is the relationship curve between the goethite content (as listed in Table 6) and physical properties index (as listed in Table 1) of lateritic clay. It can be seen from Figure 7(a) that the values of liquid limit (LL), plastic limit(PL) and shrinkage limits(SL) in lateritic clay decrease with the increase of goethite content, and the relationship between goethite content and Atterberg's limits mentioned

TABLE 6: Analytical results of the mineral compositions.

Mineral compositions	XRF				Total chemical analysis
	S-1(Guilin)	S-2(Liuzhou)	S-3(Laibin)	S-4(Wuming)	S-4(Wuming)
Quartz	12.26	15.02	41.26	0	0
Kaolinite	71.13	70.60	46.79	78.43	77.98
Gibbsite	0	0	0	12.08	12.39
Goethite	16.52	14.30	11.84	9.49	9.63

TABLE 7: Error analysis of calculation results by Bogue's method.

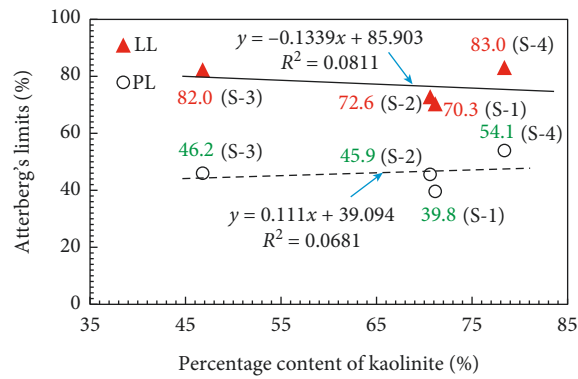| Mineral compositions	XRF				Total chemical analysis
	S-1(Guilin)	S-2(Liuzhou)	S-3(Laibin)	S-4(Wuming)	S-4(Wuming)
SiO_2	41.96	42.60	58.61	36.48	36.27
Al_2O_3	0	0	0	37.32	37.71
Al_2O_3 calculated from SiO_2 content	—	—	—	38.91	38.93
SiO_2 calculated from Al_2O_3 content	45.35	47.86	63.03	—	—
Difference	3.39	5.26	4.42	1.59	1.22

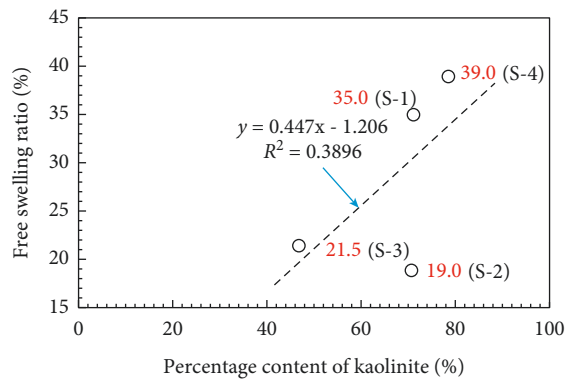FIGURE 5: Relationships between kaolinite content and Atterbeg's limits of lateritic clay.

FIGURE 6: Relationship between kaolinite content and free swelling ratio of lateritic clay.

above is basically linear. It can be seen from Figure 7(b) that the shrinkage coefficient increases with increase of goethite content, but the correlation is weak comparatively. Tan [40] analyzed the particularity of lateritic clay from the perspective of microstructure and found that free iron oxide has cementation effect on clay particles. It usually exists in lateritic clay in the form of goethite, which makes the basic unit agglomerate and fills the pores between clay particles.

Therefore, with the increase of goethite content, the adsorption capacity of soil particles to water decreases, the water loss rate accelerates and the shrinkage coefficient increases. At the same time, the porosity of clay decreases, the content of "inert water" in pores decreases, and the liquid and plastic limits of lateritic clay decrease. However, the shrinkage characteristics of lateritic clay are not only related to goethite, but also affected by the connection mode
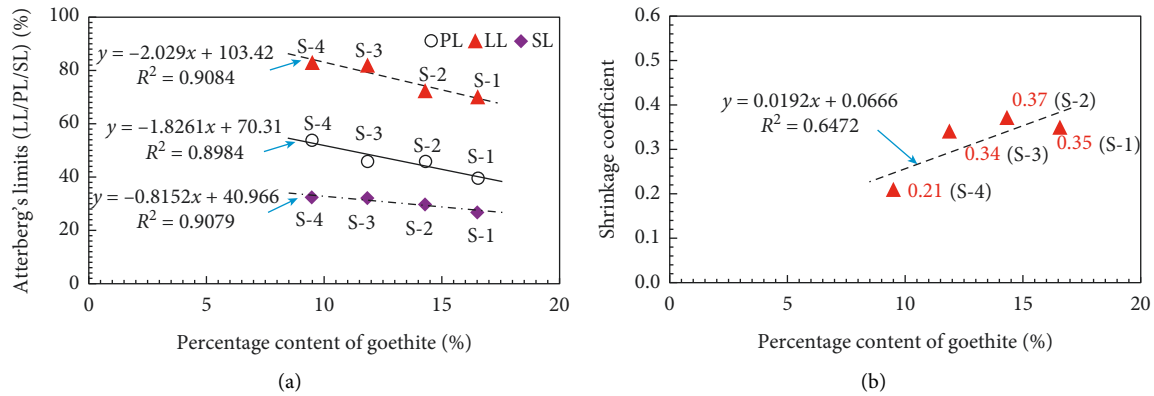
FIGURE 7: Relationships between goethite and physical properties of lateritic clay. (a) Relationship between goethite content and Atterberg's limits. (b) Relationship between goethite content and shrinkage coefficient.

between particles, the concentration of pore solution, initial moisture content and other factors, so the correlation between goethite content and shrinkage index is weak.

5. Conclusion

(1) The mineral types in lateritic clay can be preliminarily determined by differential thermal analysis (DTA) and X-ray diffraction (XDR) experiments. The experimental results show that the mineral components in lateritic clay are mainly kaolinite and goethite.

(2) By comparing and analyzing the commonly used quantitative analysis methods, the quantitative analysis method of mineral composition of Guangxi lateritic clay is determined: firstly, the content of chemical elements is determined by X-fluorescence analysis or total chemical element analysis, and then the quantitative analysis of mineral composition is completed by Bogue method according to the chemical elements of soil samples, which provides a more reliable method for the quantitative analysis of mineral composition of soil samples in this area.

(3) The physical properties of lateritic clay are mainly affected by clay minerals and cementing materials: the higher the content of clay minerals which has strong adsorption capacity for water, and the greater the corresponding liquid and plastic limits. Lateritic clay is dominated by kaolinite minerals with low adsorption capacity. Due to the existence of "inert water" in soil pores, lateritic clay also has high liquid and plastic limits. The liquid and plastic limits of lateritic clay decrease linearly with the increase of goethite, but goethite has little effect on the shrinkage characteristics. The author speculates that the shrinkage characteristics of lateritic clay may also be affected by other factors such as the connection mode between soil particles, pore solution concentration, initial water content and so on.

Data Availability

The data presented in this study are available on request from the first author or the corresponding author.

Conflicts of Interest

The authors declare that they have no conflicts of interest.

Authors' Contributions

C.-L. Y. and C. C. curated the data; Y.-F. W. was in-charge of investigation; H.-Y. M. supervised the study; E.-J. Y. wrote the original draft; S.-S. Z. wrote, reviewed, and edited the paper. All authors have read and agreed to the published version of the manuscript.

Acknowledgments

References

[1] Z. Zeng, Y. Zhao, H. Lu, and C. Wei, "Experimental performance study of ground-coupled heat pump system for cooling and heating provision in karst region," *Energy and Buildings*, vol. 158, pp. 971–986, 2018.

[2] W. Y. Jiang, *Study on Soil Characteristics and Filling Performance of Guangxi Red clay*, Guangxi University, Nanning, China, 2015.

[3] Y. W. Zhao, L. W. Kong, A. G. Guo, and Y. F. Tuo, "Mechanical behaviors and water-sensitive properties of intact Guangxi laterite," *Rock and Soil Mechanics*, vol. 24, no. 4, pp. 568–572, 2003.

[4] D. A. Sun, W. J. Liu, and H. B. Lu, "Soil-water characteristic curve of Guilin lateritic clay," *Rock and Soil Mechanics*, vol. 35, no. 12, pp. 3345–3351, 2014.

[5] Y. Xu, Z. Zeng, D. Sun, and H. Lu, "Comparative study on thermal properties of undisturbed and compacted lateritic soils subjected to drying and wetting," *Engineering Geology*, vol. 277, Article ID 105800, 2020.

[6] B. Yuan, Z. Li, Z. Zhao, H. Ni, Z. Su, and Z. Li, "Experimental study of displacement field of layered soils surrounding laterally loaded pile based on Transparent Soil," *Journal of Soils and Sediments*, vol. 21, no. 9, pp. 3072–3083, 2021.

[7] B. X. Yuan, Z. H. Li, Z. L. Su, Q. Z. Luo, M. J. Chen, and Z. Q. Zhao, "Sensitivity of multistage fill slope based on finite element model," *Advances in Civil Engineering*, vol. 2021, Article ID 6622936, 13 pages, 2021.

[8] K. Norrish, "Crystalline swelling of montmorillonite: manner of swelling of montmorillonite," *Nature*, vol. 173, no. 4397, pp. 256-257, 1954.

[9] L. R. Tan, "Study on mechanism of expansion and shrinkage of the montmorillonite crystal," *Rock and Soil Mechanics*, vol. 18, no. 3, pp. 13–18, 1997.

[10] L. R. Tan and L. W. Kong, "Study on the swelling and shrinkage of montmorillonite crystal and its relationship with matrix suction," *Science in China*, vol. 31, no. 2, pp. 119–126, 2001.

[11] J. Z. Wang, "The effects of free iron oxides on the engineering properties of lateritic clay," *Chinese Journal of Geotechnical Engineering*, vol. 5, no. 1, pp. 147–156, 1983.

[12] L. W. Kong, H. X. Luo, and J. X. Yuan, "Preliminary study on the effective cementation characteristics of the lateritic clay," *Chinese Journal of Geotechnical Engineering*, vol. 17, no. 5, pp. 42–47, 1995.

[13] R. M. Madu, "An investigation into the geotechnical and engineering properties of some laterites of Eastern Nigeria," *Engineering Geology*, vol. 11, no. 2, pp. 101–125, 1997.

[14] M. N. Arca and S. B. Weed, "Soil aggregation and porosity in relation to contents of free iron oxide and clay," *Soil Science*, vol. 101, no. 3, pp. 164–170, 1966.

[15] H. X. Luo, "The effect of amorphous materials on the mechanical property and structure of soil," *Rock and Soil Mechanics*, vol. 4, no. 1, pp. 69–74, 1983.

[16] G. R. Gao, *Neoteric Soil Geotechnology*, Science Press, Beijing, China, 2013.

[17] Z. Zeng, H. Lu, Y. Zhao, and Y. Qin, "Analysis of the mineral compositions of swell-shrink clays from Guangxi province, China," *Clays and Clay Minerals*, vol. 68, no. 2, pp. 161–174, 2020.

[18] L. R. Tan, "Quantitative analysis of clay minerals," *Acta Minaralogica Sinica*, vol. 4, no. 4, pp. 71–77, 1984.

[19] R. K. Zhang and G. Fan, "Quantitative analytic method and experiments of X-ray diffraction period of clay minerals," *Uranium Geology*, vol. 19, no. 3, pp. 180–185, 2003.

[20] S. B. Dai, J. Huang, and L. Xia, "Analysis of mineral composition and chemical components of expansive soil in North Hubei," *Rock and Soil Mechanics*, vol. 26, no. 1, pp. 300–303, 2005.

[21] Y. F. Wang, *The Influence of Mineral Component of Physical Properties of Swell-Shrink Soil of Guangxi*, Guangxi University, Nanning, China, 2011.

[22] National Development and Reform Commission (NDRC) of the People's Republic of China, *Code for Chemical Analysis Test of Rock and Soil for Hydropower and Water Conservancy Engineering (DL/T 5357-2006)*, China Electric Power Press, Beijing, China, 2006.

[23] ASTM D 7928-16, *Standard Test Method for Particle -Size Distribution (Gradation) of Fine-Grained Soils Using the Sedimentation (Hydrometer) Analysis*, New york, NY, USA, 2016.

[24] L. P. Aldridge, "Accuracy and precision of phase analysis in Portland cement by Bogue, microscopic and X-ray diffraction methods," *Cement and Concrete Research*, vol. 12, no. 3, pp. 381–398, 1982.

[25] B. L. Huang, *Mineral Identification Manual of Differential Thermal Analysis*, Science Press, Beijing, China, 1987.

[26] M. M. Duane and C. R. Robert, *X-Ray Diffraction and the Identification and Analysis of Clay Minerals*, Oxford University Press, Oxford New York, 1997.

[27] C. G. Zhao and B. Bai, *Fundamentals of Soil Mechanics*, Tsinghua University Press, Beijing, China, 2009.

[28] J. K. Mitchell and K. Soga, *Fundamentals of Soil Behavior*, John Wiley, New York, NY, USA, 3rd edition, 2005.

[29] Y. Xu, D. a. Sun, Z. Zeng, and H. Lu, "Temperature dependence of apparent thermal conductivity of compacted bentonites as buffer material for high-level radioactive waste repository," *Applied Clay Science*, vol. 174, pp. 10–14, 2019.

[30] X. Zhou, L. He, and D. Sun, "Three-dimensional thermal modeling and dimensioning design in the nuclear waste repository," *International Journal for Numerical and Analytical Methods in Geomechanics*, vol. 46, no. 4, pp. 779–797, 2022.

[31] Z. Zeng, X. Zhang, Y. Zhao, and H. Lu, "Performance of a ground-source heat pump system and the heat-moisture migration of surrounding soils in karst areas," *Journal of Performance of Constructed Facilities*, vol. 31, no. 5, Article ID 04017050, 16 pages, 2017.

[32] Y. Xu, D. Sun, Z. Zeng, and H. Lu, "Effect of temperature on thermal conductivity of lateritic clays over a wide temperature range," *International Journal of Heat and Mass Transfer*, vol. 138, pp. 562–570, 2019.

[33] Y. Tan, X. Xu, H. Ming, and D. a. Sun, "Analysis of double-layered buffer in high-level waste repository," *Annals of Nuclear Energy*, vol. 165, Article ID 108660, 2022.

[34] L. S. Donald, *Soil Physical Chemistry*, CRC Press LLC, New York, NY, USA, 2nd edition, 1999.

[35] R. N. Yong and B. P. Warkentin, *Introduction to Soil Behavior*, The Macmillan Company, New York, NY, USA, 1966.

[36] S. L. Li, Z. Z. Bo, and S. J. Qin, *Translation Anthology of Absorbed Water in Soils*, Geological Publishing House, Beijing, China, 1982.

[37] G. X. Li, *Advanced Soil Mechanics*, Tsinghua University Press, Beijing, China, 2004.

[38] W. Y. Yun, *Testing Study on Absorbed Water in Expansive and Shrinkable Soil*, Guilin University of Technology, Guilin, China, 2019.

[39] S. Y. Xue and F. Z. Bian, "Structure and engineering characteristics of lateritic clay," *Chinese Journal of Geotechnical Engineering*, vol. 9, no. 3, pp. 94–106, 1987.

[40] L. R. Tan, "The microscopic foundation of properties of lateritic clay," in *Proceedings of the 3rd National Engineering Geological Conference*Chengdu University of Science and Technology Press, Chengdu, China, 1988.